PARETO OPTIMIZATION FOR FOUR-DIMENSIONAL WAVE REFRACTION SIMULATION FROM SENTINEL-1A

Maged Marghany and Shattri Mansor
Geospatial Information Science Research
Centre, Faculty of Engineering
University Putra Malaysia
43400 UPM, Serdang, Selangor
Email :magedupm@hotmail.com

KEY WORDS: 4-D B-spline algorithm, Sentinel-1A data, wave refraction, 4-D wave refraction pattern, Pareto optimization.

ABSTRACT: The quantitative descriptors of the ocean surface wave properties such as wave height and wave slope spectra can retrieve from several satellite SAR missions, such as Sentinel-1A data. The retrieving techniques of sea surface quantitative descriptors involve linear and nonlinear techniques. This study presents a new approach for the simulation of four-dimensional wave refraction pattern in Sentinel-1A data. In doing so, the quasi-linear used to model significant wave height based on the new approach of the 4-D B-spline azimuth cut-off algorithm. The study shows that wave refraction pattern can simulate from Sentinel-1A data with convergence and divergence, respectively. In conclusion, modification of the conventional azimuth cut-off algorithm can be used to retrieve significant wave height in Sentinel-1A data under circumstances of Pareto optimization of wave transformation using 4-D B-spline algorithm.

1. INTRODUCTION

Yet there is no study on 4-D wave refraction from Synthetic Aperture Radar (SAR). The wave spectra parameters retrieving are restricted to two concepts which are (i) linear and (ii) nonlinear (Beal et al., 1983, Hasselmann and Hasselmann, 1991, Vachon et al. 1994; Forget and Brochel 1995). These two concepts are not able to retrieve accurate wave spectra parameters. As the retrieving of wave spectra from SAR is mainly influenced by nonlinearity besides the deformation of wave geometry in SAR images due to shadowing and speckles effects too. With this regard, SAR sensors are still not fully operational for wave spectra studies.

Wave refraction plays tremendous directive for shoreline configuration. This can be presented in both convergence and divergence that can cause erosion and sedimentation, respectively. Wave refraction simulation is required standard algorithms to reconstruct its accurate pattern. Consequently, the simulation of wave refection pattern from retrieved wave spectra parameters will experience with several limitations: (i) ambiguity in direction; (ii) nonlinearity due velocity bunching and (iii) the retrieved significant wave height based azimuth cut-off could be constant through the SAR image. In fact, 2-D FFT can be applied on SAR data with window kernel size of 512 x 512 pixels and lines. This means that the estimated wavelength from 2-DFFT cannot be less than 50 m. However, the wave spectra experience shrinking on their wavelength as they are approaching the shallow water. With this regard, the simulated SAR image spectrum must be turned out to be far from the real wave spectrum and rather complicated post-processing is necessary for extracting quantitative wave information.

There are many attempts to turn on the SAR wave spectra into real wave spectra by using inverse spectra method as documented on Schulz-Stellenfleth et al., (2007). Further, empirical algorithms are used to retrieve deep water significant wave height independent from wave model input. Pleskachevsky et al., (2015), recently implemented the statistical analysis to compared between, input model i.e. CWAM, buoy, and significant wave height was retrieved from TS-X image. However, this procedure involves errors of uncertainty of peak wave period, the comparative weighting of dissimilar spectral peaks, and the wind input of the CWAM model. With this regard, the novelty of this work is to optimize the errors occurring on retrieving wave spectra parameter from SAR data. The main hypotheses is 4-D wave spectra are encoded in 3-D wave spectra as 2-D wave spectra are encoded in 1-D wave spectra. The main objective is to simulate 4-D of wave refraction pattern from Sentinel-1A.

2. DATA ACQUISITION

The data used within 4-D wave spectra retrieving are (i) SAR data which is Sentinel-1 A; and (ii) and the real in-situ wave measurement during Sentinel-1 A overpassed.

2.1. Sentinel-1 Data

In this study, Sentinel-1 A data with single polarization VV have been used. Sentinel-1 is the European Radar Observatory, representing the first new space component of the GMES (Global Monitoring for Environment and Security) satellite family, designed and developed by ESA and funded by the EC (European Commission). Sentinel-1 is composed of a constellation of two satellites, Sentinel-1A (Figure 1) and Sentinel-1B, sharing the same orbital plane with a 180° orbital phasing difference.

Except for the ocean wave and current studies, which is a single polarization mode (HH or VV) with C-band, the SAR instrument has to support operations in dual polarization (HH-HV, VV-VH), requiring the implementation of one transmit chain (switchable to H or V) and two parallel receive chains for H and V polarization. The specific needs of the four different measurement modes with respect to antenna agility require the implementation of an active phased array antenna. For each swath the antenna has to be configured to generate a beam with fixed azimuth and elevation pointing. Appropriate elevation beamforming has to be applied for range ambiguity suppression. In addition, the incident angle is ranged between 20º-46º.

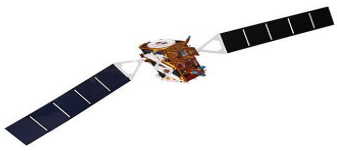

Figure 1. Sentinel-1 A satellite.

2.2. In situ ocean wave measurement

The in situ wave spectra quantities i.e. wavelength, significant wave height, wave period, wave velocity, and direction, are obtained using Acoustic Wave and Current (AWAC) (Figure 2) from the east coast of Kuala Terengganu, Malaysia on March 8th till 12th March 2015, at 5°28'02" N and 103°07'48"E (Figure 3). AWAC recorded the water column current speed and directions.

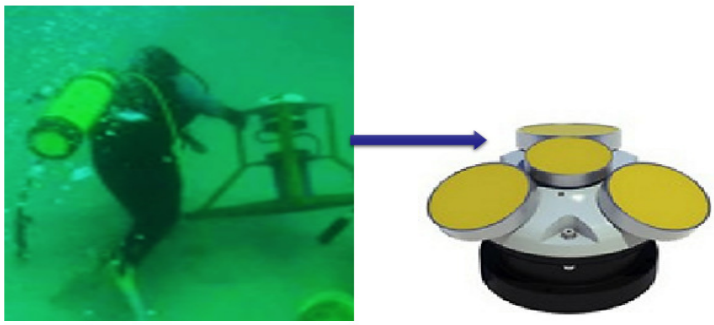

Figure 2. In-situ wave spectra measurements by AWAC

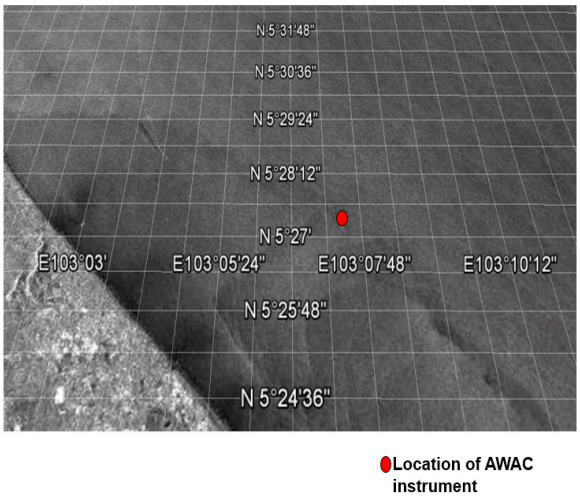

Figure 3. Geographical location of AWAC instrument.

3. MODEL

3.1. Quasi-linear Model

To map observed Sentinel-1A spectra into the ocean wave spectra, a quasi-linear model was applied. The simplified quasi-linear theory is explained below: according to the Gaussian linear theory, the relation between ocean wave spectra $S(\vec{K},\phi)$ and AIRSAR image spectra $S_Q(\vec{K})$ could be described by tilt and hydrodynamic modulation (real aperture radar (RAR) modulation). The tilt modulation is linear to the local surface slope in the range direction i.e. in the plane of radar illumination. The tilt modulation in general is a function of wind stress and wind direction for ocean waves and Sentinel-1 A. According to Vachon et al., (1994) the tilt modulation is the largest for HH polarization. Alpers et al., (1981) and Alpers and Bruning (1986) reported that hydrodynamic interaction between the scattering waves (ripples) and longer gravity waves produced a concentration of the scatterer on the up wind face of the swell. In order to estimate the significant wave height from the quasi-linear transform, we adopted the algorithm that was given by Marghany (2003) to be appropriate for the geophysical conditions of tropical coastal waters:

$$\lambda_c = \beta\left(\int_{H_{s_0}}^{H_{s_n}} \sqrt{H_s}\, dH_s + \int_{U_0}^{U_n} \sqrt{U}\, dU\right) \qquad (1)$$

where λ_c is cut-off azimuth wavelength, H_s and U are the in situ data of significant wave height and wind speed along the coastal waters of Kuala Terengganu, Malaysia. The measured wind speed was estimated at 10 m height above the sea surface. The changes of significant wave height and wind speed along the azimuth direction are replaced by dH_s and dU, respectively. The subscript zero refers to the average in situ wave data collected before flight pass over by two hours while the subscripts n refers to the average of in situ wave data during flight pass over the study area. β is an empirical value which results of R/V multiplied by the intercept of azimuth cut-off (c) when the significant wave height and the wind speed equal zero. A least squares fit was used to find the correlation coefficient between cut-off wavelength and the one calculated directly from the Sentinel-1 A spectra image by equation (1). Then, the following equation was adopted by Marghany (2001) and (2003) to estimate the significant wave height (H_{sT}) from the Sentinel-1 A images

$$H_{sT} = \beta^{-2} \int_{\lambda_{c_0}}^{\lambda_{c_n}} (\lambda_c)^2\, d\lambda_c \cdot \qquad (2)$$

where β is the value of $\left(c\frac{R}{V}\right)^{-1}$ and H_{sT} is the significant wave height simulated from Sentinel-1 A images. The introduced method (azimuthally cut off) is designed for homogeneous wave fields as waves can be found over the open ocean under deep water condition with homogeneous bathymetry. A linear wave transform model can be used to solve the problem of homogeneous wave fields by simulating the physical wave parameters nearshore.

The wave refraction model over the Sentinel-1A image is formulated on the basis of wave number and wave energy conversation principle, gentle bathymetry slope, steady wave conditions and only depth refractive. It can be modified the significant wave height (Hasselmann and Hasselmann (1991) and Herbers et al (1999), due to refraction into 4-D as follows:

$$E(\vec{K}, H_S, t) = S(k_x, k_y, k_z, k_t)\, p(H_S) \qquad (7)$$

Where $S(k_x, k_y, k_z, k_t)$ is the distribution for the wave number and $p(H_S)$ is the probability distribution of the significant wave height in 4-D.

3.2. 4-D Wave Refraction Simulation

Let us consider a volume as a subset of 3D space with an additional scalar value given in each of its points. If this scalar value is interpreted as an additional point coordinate, the volume becomes a 4D "height field" or a hypersurface in 4D space. The defined scalar field can be thought of as a variable of the object's density, temperature, etc. Scalar values can be specified in the nodes of a regular space grid (voxel data) or by a continuous function of three variables (so-called implicit surface model or more generally the function representation. Albeit normal thought of space as three-dimensional, any object can be drive in the space of four and even higher dimensions. The main challenge is to determine logic methods to reconstruct such high-dimensional stuffs. This section exploits 4D spline to reconstruct 4-D of Sentinel-1A data. Let *u*, *v*, and *w* are constrained to the interval *u, v, w* $\in$ [0, 1] and S(*u, v, w, t*) $\in$(*x, y, z*). This means that the object is divided into hyperpatches. The hyperpatches are represented using surfaces and curves. Then the surface defined by setting one of *u, v, w* to a constant integer value which is yelled a knot plane which are the defining the surfaces of hyperpatches (Mortenson 1985). The points in the interior and on the boundary of the parametric solid is given by (Mortenson 1985),

$$p(u,v,w) = [x\ y\ z] = [x(u,v,w) \quad y((u,v,w) \quad z(u,v,w)] \qquad (8.0)$$

To implement the 4-D spline, the wave spectra parameters which are assimilated at individually knot time and knot planes become temporal functions. Then wave spectra pattern can be expressed in 4D B-spline model as (Amini et al., 1998):

$$S(u,v,w,t) = \sum_{i=1}^{I}\sum_{j=1}^{J}\sum_{k=1}^{K}\sum_{l=1}^{L} E(\vec{K}, H_S, t) O_i(u) O_j(v) O_k(w) O_l(t) \qquad (9.0)$$

where $O_i(u)$, $O_j(v)$, $O_k(w)$, and $O_l(t)$ are B-spline basis functions which blend control points of $E(\vec{K}, H_S, t)$ and $(I \times J \times K \times L)$ is the total number of model control points. By changing the order of B-spline summation, a more effective method to retrieve a multi-dimensional B-spline wave spectra refraction model results.

3.3. Pareto Optimal Solution

In this research, two objectives are considered. One is retrieved significant wave height from SAR data and the other is 4-D spline for wave refraction. Pareto optimal solutions are applied to optimize the 4-D wave refraction variation in SAR image. In this problem, the chromosome consists of a number of genes where every gene corresponds to a coefficient in the nth-order surface fitting polynomial as given by

$$f(S_{i,j,k,t}) = S_0 + S_1 i + S_2 j + S_3 k + S_4 t + \ldots + S_m t^n \qquad (10)$$

where S [*0,1.....m*] are the wave refraction parameter coefficients that will be estimated by the genetic algorithm to approximate the minimum error for wave refraction parameters. *i,j,k* and *t* are indices of the pixel location in 4-D image respectively, *m* is the number of coefficients.

Then the weighted sum to combine multiple objectives into single objective is given by

$$f(S) = w_1 f_1(S) + w_2 f_2(S) + \cdots + w_n f_n(S) \qquad (11)$$

where $f_1(S), f_2(S), \ldots, f_n(S)$ are the objective functions and $w_1, w_2, \ldots, w_n$ are the weights of corresponding objectives that satisfy the following conditions.

$$w_i \geq 0 \quad \forall i = 1,2,...,n$$
$$w_1 + w_2 + ... + w_n = 1 \tag{12}$$

Once the weights are determined, the searching direction is fixed. To search Pareto optimal solutions as much as possible, the searching directions should be changed again and again to sweep over the whole solution space.

4. RESULTS AND DISCUSSION

Figure 4 shows the wavelength spectra which derived from Sentinel-1A image are ranged between 50 m to 200 m with 180° ambiguity. The spectra peak indicates northeast wave spectra propagation along the coastal water of Malaysia. In fact, March is representing northeast monsoon season as wave propagated from the northeast toward the east coast of Malaysia. This agrees with studies of Wrytki, K. (1961); Wong (1981) ; Zelina et al., (2000); Marghany (2004); Marghany (2003) and Marghany et al., (2011).

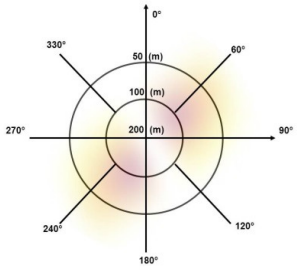

Figure 4. Wave spectra derived from Sentinel-1A image.

Figure 5 shows the 4-D wave refraction pattern which derived from 4-D B-spline based Pareto optimal solutions algorithm. 4-D wave refraction pattern shows clear convergence and divergence zone along the coastal water. The divergence zone dominated by breaking significant wave height of 2 m while the convergence zone is dominated by breaking significant wave height of 3.5 m. Moreover, four-dimensional of spectra energy indicates that the convergence zone dominated by highest refractive index of 2.8. In additions, 4-D suggests a turbulent pattern flow which is noticeable by asymmetrical pattern either in convergence or divergence zone (Figur 5b).

(a) **(b)**

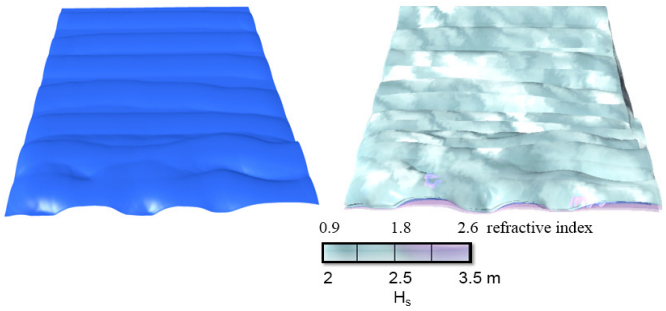

Figure 5. Wave refraction (a) 3-D and (b) 4-D.

The energy of 4-D spline is demarcated as the quantity of separately knots energy that is pronounced as the integral of the matching apparent which is ended to the knot plane surface (Waks et al., 1996). All knot planes are optimized although the hypothetical function are fragmented. The 4-D algorithm procedure is ended meanwhile the length is shorter than the threshold. Finally, the implementation of Pareto optimal solution improved the 4-D visualization of the wave refraction pattern. Indeed, Pareto-front contains the Pareto-optimal solutions and in case of continuous front, it divides the objective function space into two parts, which are non-optimal solutions and infeasible solutions. With this regard, it improved the robustness of pattern search and improved the convergence speed of 4-D B-spline algorithm. This agrees with the study of Yudong et al., (2013).

5. CONCLUSION

This study has demonstrated a new approach for simulation of wave refraction pattern from Sentinel-1A data. In doing so, the quasi-linear exploited to model significant wave height based on the new advance of the 4-D B-spline

algorithm. The study shows that wave refraction pattern can simulate from Sentinel-1A data with convergence and divergence spectra energy. In conclusion, 4-D wave refraction pattern in spite of nonlinearity between actual ocean wave spectra and Sentinel-1A data can be simulated by 4-D B-spline algorithm based on Pareto optimization.

References

Alpers, W.R., Ross D.B., Rufenach C.L., (1981). On the detectability of ocean surface waves by real and synthetic aperture radar. *Journal of Geophysical Research* 83, 6481-6498.

Alpers, W., and Bruning C., (1986). On the relative importance of motion-related contributions to SAR imaging mechanism of ocean surface waves. *IEEE Transactions on Geoscience and Remote Sensing* 24, 873-885.

Amini, A.A., Y. Chen, R. W. Curwen, V. Mani, and J. Sun, 1998a, Coupled B-Snake Grids and Constrained Thin-Plate Splines for Analysis of 2-D Tissue Deformations from Tagged MRI", IEEE Transactions on Medical Imaging, 17(3):344-356.

Beal., R.C., Tilley, D.G., Monaldo, F.M., (1983). Large-and small-scale spatial evolution of digitally processed ocean wave spectra from seasat synthetic aperture Radar. *Journal of Geophysical Research* 88, 1761-1778.

Forget, F., Broche, P., Cuq, F., (1995). Principles of swell measurement by SAR with application to ERS-1 observations off the Mauritanian coast. *International Journal of Remote Sensing* 16, 2403-2422.

Herbers, T. H. C., S. Elgar and R. T. Guza (1999). Directional spreading of waves in the nearshore, *Journal of Geophysical Research*, **104**, 7683-7693.

Hasselmann, K., Hasselmann S., (1991). On the nonlinear mapping of an ocean spectrum and its inversion". *Journal of Geophysical Research,* **96**, 10,713-10,799.

Li, X., S. Lehner, W. Rosenthal (2010). "Investigation of Ocean Surface Wave Refraction Using TerraSAR-X Data". IEEE Tran. Geos. Rem. Sens. Vol.48,pp.830—840.

Marghany M., (2001). TOPSAR Wave Spectra Model and Coastal Erosion Detection". *International Journal of Applied Earth Observation and Geoinformation*. (3):357-365.

Marghany M., (2003).ERS-1 modulation transfer function impact on shoreline change. *International Journal of Applied Earth Observation and Geoinformation*. (4):279-294.

Marghany M. (2004). "Velocity Bunching Model for Modelling Wave Spectra along East Coast of Malaysia". J. Ind. Soc. Rem. Sens., 32,185-198.

Marghany,M. (2011). Modelling shoreline rate of changes using holographic interferometry. International Journal of the Physical Sciences. Vol. 6(34), pp. 7694 – 7698.

Marghany,M., Mazlan Hashim, and A.P. Cracknell (2011).Simulation of shoreline change using AIRSAR and POLSAR C-band data. Environmental Earth Sciences. 64:1177–1189.

Schulz-Stellenfleth, J., König, T., Lehner, S., 2007. An empirical approach for the retrieval of integral ocean wave parameters from synthetic aperture radar data. J. Geophys. Res. 112, C03019.

Pleskachevsky, A., Gebhardt, C., Rosenthal, W., Lehner, S.,Hoffmann, P., Kieser, J., Bruns, T., Lindenthal, A., Jansen, F., Behrens, A., 2015. Satellite-based radar measurements for validation of high-resolution sea state forecast models in the German Bight. Int. Arch. Photogramm. Remote Sens. Spatial Inf. Sci., XL-7/W3 983–990.

Vachon P.W., K.E. Harold and J. Scott. (1994). Airborne and Space-borne Synthetic Aperture Radar Observations of ocean waves. *Journal of Atmospheric.-Ocean* 32 (10) ; 83-112.

Vachon P.W., A. K. Liu and F.C. Jackson.- 1995. Near-Shore Wave Evolution Observed by Airborne SAR During SWADE. *Journal of Atmospheric.-Ocean* , 2: 363-381.

Vachon, P.W. and J.W.M. Campbell and F.W. Dobson.(1997). Comparison of ERS and Radarsat SARS for Wind and Wave Measurement. *Paper Presented at 3rd ERS Symposium (ESA)* 18-21 March, 1997. Florence, Italy.

Waks, E., Prince, J., Douglas, A 1996. Cardiac Motion Simulator for Tagged MRI. Mathematical Methods in Biomedical Image Analysis , 182–191.

Yudong Z, Shuihua W., Genlin J. and Zhengchao D., 2013. Genetic Pattern Search and Its Application to Brain

Image Classification. Math. Prob. in Eng., 1-8.

Wyrtki,K., (1969). Physical Oceanography of the South-East Asian Waters". *In NAGA Report* Vol. 2, Univ. Calif Scripps Inst. Ocean., La Joll.

Zelina, Z. I., A. Arshad, S.C.Lee, S.B.Japar, A. T. Law, Nik Mustapha, and M. M. Maged, (2000). “East Coast of Peninsular Malaysia”. In: Seas at The Millennium: An Environmental Evaluation. Charles Sheppard (ed.). Elsevier Science LTD London, UK.